Beyond Conventional Fractional Frequency Reuse for Networks with Irregular Cell Layout: An Optimization Approach and Performance Evaluation

Lei Chen* and Di Yuan*

*Department of Science and Technology, Linköping University, SE-601 74 Norrköping, Sweden.
E-mails: leich@itn.liu.se, diyua@itn.liu.se

***Abstract*—Fractional frequency reuse (FFR) is one of the key concepts for interference mitigation in OFDMA networks. Previous work on FFR has focused on networks of relatively small size and standard hexagon-shaped cell layout. For real-life networks with very irregular cell layout and high variation in radio propagation, standard reuse schemes (e.g., reuse with a factor three) are inadequate; applying a standard scheme, if possible at all, is far from optimal due to the irregularity. We present an approach based on large-scale optimization to study FFR in networks with irregular cell layout. The approach goes beyond the conventional reuse schemes by optimizing the allocation of the cell-edge sub-band of every cell, taking into account the interference caused by the sub-band allocation of all other cells. What's more, whereas the conventional FFR scheme uses three sub-bands, our optimization process allows for considering the number of sub-bands as a parameter, and enables the analysis of the impact of this parameter on FFR performance. Performance evaluation for networks with realistic radio propagation conditions shows that the approach enables significant throughput improvement at cell-edge zones, and sometimes it is optimal to split the cell-edge band into more than the standard three sub-bands. These results along with the analysis demonstrate the potential benefits of the proposed approach in practicing FFR for large-scale networks, and illustrate the performance trade-off between the cell-edge and cell-center zones.**

***Keywords* – Fractional frequency reuse, optimization**

I. Introduction

A. Background

Orthogonal Frequency Division Multiple Access (OFDMA) is a very promising technology for high speed wireless networks. It has been adopted in the air interface of 3GPP Long Term Evolution (LTE) [1] and IEEE 802.16 WiMAX [2] systems. By OFDMA, the spectrum into a large number of sub-carriers. Being orthogonal to each other, each of the sub-carriers is modulated independently of the others to carry a low rate data stream. OFDMA is inherently robust against multipath fading. Moreover, it admits very flexible bandwidth usage and high spectrum efficiency.

One performance engineering issue in OFDMA networks is interference control and mitigation. With OFDMA, intra-cell interference is not present. Inter-cell interference, on the other hand, may become a performance-limiting factor at some parts of a network. Reusing all sub-carriers in all cells, i.e., reuse with factor one (reuse-1), typically gives the best performance in terms of the overall system throughput [3]. However, cell-edge users may suffer severely in this scheme, because the data throughput of users at cell-edge zones are very interference-sensitive. On the other hand, higher order reuse schemes, such as a reuse factor of three, can be used to limit the interference and improve the throughput of cell edge, but this will cause huge loss of bandwidth and bring down significantly the overall throughput.

To balance the cell-edge throughput and the overall one, Fractional Frequency Reuse (FFR) has been proposed [4, 5, 6, 7]. FFR is supported in both LTE and WiMAX network standards. By this concept, a cell is split into two zones: center and edge. The frequency spectrum is correspondingly partitioned into two parts. One is reused with factor one for all cell-center users. The second part is further divided into several sub-bands; each cell is allocated one of the sub-bands for its cell-edge zone. As the cell-edge sub-bands have a higher reuse factor (typically three), significant interference reduction and thereby higher throughput are achieved for users at cell edge.

B. Contributions

An increasing amount of research has been devoted to FFR recently. Its performance has been analyzed in [8, 9, 10, 11, 12, 13, 14]. In [15, 16, 17], some variations of FFR have been proposed and examined. The investigation in this paper is carried out in view of the following aspects.

- Most of the analysis up to date focus on networks of relatively small size with regular hexagonally shaped cells. For this cell layout, a straightforward application of the reuse-3 scheme is the best choice. An underlying assumption is that cells have an equal number of adjacent cells, all generating the same amount of interference. This assumption does not hold for real-life networks, for which standard schemes become inadequate.
- For networks with irregular cell layout, standard schemes may fail not only because it may give poor performance, but also because it can not be applied directly. In fact, in many cases it is very difficult to derive a sub-band reuse pattern from standard schemes at all, as the number of significant interferers varies by cell.
- There is a need of approaches for planning and evaluating FFR in large scale networks. Note that small cell structure with a wrap-around signal propagation model will scale only if there is a structural pattern in radio propagation. In

Digital Object Identifier: 10.4108/ICST.WICON2010.8616
http://dx.doi.org/10.4108/ICST.WICON2010.8616

a real, large-scale network with a very irregular cell layout, the performance should be investigated by considering the network in its entirety. In this case, full-scale system simulation is often not feasible, and approaches enabling fast performance assessment is highly desirable.

- Previous research has not investigated the impact of the number of sub-bands (given a fixed-sized spectrum) on FFR performance, except using the standard three sub-bands in hexagon cells. Under realistic radio propagation and a network-specific cell layout, three sub-bands is not necessarily the best choice, and the optimal number of sub-bands becomes an issue in its own right.

To this end, the research in this paper provides novel approach and analysis to shed light on the answer to the following question: *How to plan FFR, both in terms of sub-band allocation and the number of sub-bands, under realistic interference scenarios to optimize cell-edge performance, and how much performance improvement to expect?*

To address the question, we apply a large-scale optimization approach. First, we define a metric to evaluate any given FFR sub-band allocation. In our approach, the service area is represented by a large number of pixels. For each pixel of the cell edge zones, the performance is measured by the achievable data rate, when all the interfering cells are active. Together, the values form a throughput map over the edge zones, allowing for fast assessment of FFR performance without having to restrict to any particular scheduling assumption. For sub-band allocation, our approach does not use any regular reuse pattern. Instead, a search algorithm is applied to find the allocation of the sub-bands to the cell-edge zones. For the edge zone of each cell, the optimization takes into account the interference from all other cells. As a result, the optimized reuse pattern is, similar to cell layout, also irregular. The search algorithm consists in two phases. The first phase constructs an initial reuse pattern. In the second phase, the algorithm searches for improvements by changing the sub-band of every individual cell, or swapping the sub-bands of cell pairs.

Our optimization framework and solution algorithm allow for optimizing FFR performance in large-scale networks. In addition, they can be used to find out, for a given cell-edge spectrum, how many sub-bands should be created for FFR. Indeed, our results show that splitting the cell-edge band into more than three sub-bands may give better performance. We present experimental results for networks with realistic radio propagation conditions. The results and performance analysis demonstrate the potential of our optimization approach for planning FFR in real-life networks.

For FFR, the performance gain at cell edge comes at the price of throughput degradation in the cell-center zones. Our experimental results illustrate this trade-off, in addition to demonstrating the optimization approach itself. Moreover, the results shows that the expected performance is highly sensitive to the percentage of area considered as cell edge, thus the definition of cell edge plays a crucial role in FFR.

C. Paper Organization

The remainder of the paper is organized as follows. In Section II, we provide the system model and justify the performance metric that we use. The resulting optimization problem and solution algorithm are presented in Section III. In Section IV we provide results of performance evaluation of FFR optimization for realistic and large-scale network scenarios, and illustrate the pros and cons of FFR. Concluding remarks and a discussion of further investigations are given in Section V.

II. System Model

A. Conventional FFR

FFR combines reuse-1 and a higher order reuse scheme; the latter intends to improve performance at cell edge. A standard FFR scheme for cells of hexagonal shape is illustrated in Figure 1 [17]. Each cell is split into a center zone and an edge zone. The frequency band is divided into two parts. The center band (marked white) is used with reuse-1. The cell-edge band is further divided into three sub-bands (yellow, purple and blue). In the reuse pattern, each of the sub-bands is used by the cell edge in $1/3$ of the cells.

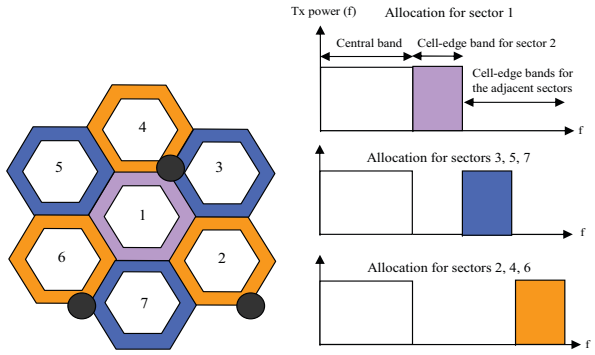

Fig. 1: An Illustration of FFR [17].

For cell center, throughput typically decreases in comparison to reuse-1 of the entire band, because of users in cell center are bandwidth-limited. At cell edge, however, users are more sensitive to interference. Hence it is very likely that less interference yields higher throughput, even if the bandwidth becomes smaller. For the cell structure in Figure 1, reuse-3, as shown in the figure, is optimal simply because it reduces the interference maximally. For realistic networks with irregular cell coverage pattern, on the other hand, no simple reuse pattern can achieve the optimal performance.

B. Network Model

Consider a large-scale multi-cell OFDMA network, and let $\mathcal{C}$ denote the set of cells. The network service area is modeled by a regular grid of a large number of pixels, denoted by set $\mathcal{J}$. A pixel $j \in \mathcal{J}$ is a small square area, within which radio propagation is considered uniform. We consider antenna of one transmitter and one receiver (SISO) in this paper, and use $g_{ij}(i \in \mathcal{C}, j \in \mathcal{J})$ to denote the total gain between cell

Digital Object Identifier: 10.4108/ICST.WICON2010.8616
http://dx.doi.org/10.4108/ICST.WICON2010.8616

antenna of i and pixel j. The gain parameter can be obtained by measurements and/or propagation predictions.

The total bandwidth of the system is denoted by B. It is split into two parts for center and edge zones The bandwidths of these two parts are denoted by B_c and B_e ($B = B_c + B_e$), respectively. The latter is further divided into sub-bands. If B_e is partitioned into K sub-bands of equal size, each will have a bandwidth $B_{sub} = \frac{B_e}{K}$. Denote the set of these sub-bands for edge zones by $\mathcal{K} = \{1, \ldots, K\}$.

Denote by p^{tot} the total downlink Tx power of a cell antenna. In the presentation, the power is uniform in all cells to simplify notation; generalization to cell-individual power is straightforward. In every cell, this power is evenly split on all sub-carriers in the cell-center band and the cell-edge sub-band. Hence at cell edge, the power over all sub-carriers equals $p_e = p^{tot}\frac{B_{sub}}{B_{sub}+B_c}$.

C. What is Cell Edge?

There is no unique definition of cell edge. Generally speaking, it is the area of a cell that is prone to interference, that is, places where the serving cell's signal is not much stronger than those of the surrounding cells. For the system model, a reasonable definition is the area (pixels in the network model) having pilot SINR below a given threshold. As a result, the size of cell-edge zones depends on the chosen pilot SINR threshold. Increasing the threshold means to include more pixels into the edge zone and let the center zone shrink in size. As will be clear later, this has a significant impact on the FFR reuse pattern and its performance.

Denote by $\mathcal{J}_i^e$ the set of cell-edge pixels having cell i as the best server, and let $\mathcal{J}^e = \cup_i \mathcal{J}_i^e$. Note that, with an irregular cell layout, the formation of cell-edge zones is irregular as well. Consequently, cell-edge zones are frequently but not necessarily located at cell border. Also, if the entire service area of a cell has good channel condition, the cell may not have any edge at all, and no sub-band needs to be allocated. Merely for the sake of simplifying notation, we assume all cells in $\mathcal{C}$ have cell edge in the algorithm presentation in Section III.

D. Sub-band Allocation and Cell-edge Throughput

In FFR, every cell is allocated a bandwidth B_c for the cell-center users (i.e., reuse-1), and one of the sub-bands of bandwidth B_{sub} for its edge (if cell edge is present). Since FFR is used for interference mitigation at cell edge, we focus on cell-edge throughput in this paper.

FFR sub-band allocation, which is the task of the optimization process in Section III, can be represented by a partition of the cells into K subsets, each containing cells that are allocated sub-band $k \in \mathcal{K}$, i.e., a tuple of subsets

$$\mathbf{c} = (\mathcal{C}_1, \ldots, \mathcal{C}_k, \ldots \mathcal{C}_K), \tag{1}$$

where $\mathcal{C}_k$ denotes the set of cells that are allocated sub-band k. For a pixel j served by cell $i \in \mathcal{C}_k$, the SINR reads

$$SINR_{ij}(\mathbf{c}) = \frac{p_e g_{ij}}{\sum_{\ell \in \mathcal{C}_k, \ell \neq i} p_e g_{\ell j} + \sigma_k^2}. \tag{2}$$

The nominator is the received power of a user in j; the denominator consists in interference from cells reusing sub-band k and the noise figure (per Hz). We assume uniformly distributed noise effect. As a result, the SINR is uniform across the sub-band.

A throughput function f translates the SINR into achievable single-user throughput. The most simple choice of f is the Shannon formula, that is,

$$f(SINR_{ij}(\mathbf{c}), j) = B_{sub} log_2(1 + SINR_{ij}(\mathbf{c})). \tag{3}$$

We would like to stress the fact that any empirical function (by simulation and/or measurements) can be used. Both the system model and the optimization process are developed for a general function f. The Shannon formula is used only for the numerical illustrations, and is purely for the sake of numerical comparability.

III. FFR OPTIMIZATION

A. Problem Characterization and Algorithm Overview

From the system model in Section II, optimizing the FFR pattern for interference mitigation amounts to finding a partition $\mathbf{c}$ to maximize the throughput of the cell-edge areas. A natural metric is the average throughput, that is

$$\max_{\mathbf{c}} \frac{1}{|\mathcal{J}^e|} \sum_{k=1}^{K} \sum_{i \in \mathcal{C}_k} \sum_{j \in \mathcal{J}_i^e} f(SINR_{ij}(\mathbf{c}), j). \tag{4}$$

The optimization problem can be stated more explicitly by the following integer programming model. The model uses two sets of variables.

$$x_{ik} = \begin{cases} 1 & \text{if cell } i \text{ uses sub-band } k, \\ 0 & \text{otherwise.} \end{cases}$$

$$y_{i\ell} = \begin{cases} 1 & \text{if cells } i \text{ and } \ell \text{ use the same sub-band,} \\ 0 & \text{otherwise.} \end{cases}$$

$$\max \frac{1}{|\mathcal{J}^e|} \sum_{i \in \mathcal{C}} \sum_{j \in \mathcal{J}_i^e} f\left(\frac{p_e g_{ij}}{\sum_{\ell \in \mathcal{C} \setminus \{i\}} p_e g_{\ell j} y_{i\ell} + \sigma_k^2}\right) \tag{5}$$

$$\text{s.t.} \sum_{k \in \mathcal{K}} x_{ik} = 1, \quad i \in \mathcal{C}, \tag{6}$$

$$x_{ik} + x_{\ell k} \leq y_{i\ell} + 1, \quad k \in \mathcal{K}, i, \ell \in \mathcal{C}, \tag{7}$$

$$x_{ik} \in \{0, 1\}, \quad i \in \mathcal{C}, k \in \mathcal{K}, \tag{8}$$

$$y_{i\ell} \in \{0, 1\}, \quad i, \ell \in \mathcal{C}. \tag{9}$$

In the above model, (6) states that each cell is allocated one sub-band in $\mathcal{K}$. Constraints (7) ensure that $y_{i\ell}$ is one, and thus the interference is taken into account in (5), if $x_{ik} = x_{\ell k} = 1$ for any k.

For the combinatorial optimization problem defined by the model, where function f may take a general form (except the restriction of being monotonously increasing), guaranteeing global optimum is difficult. Solving the integer model for

Digital Object Identifier: 10.4108/ICST.WICON2010.8616
http://dx.doi.org/10.4108/ICST.WICON2010.8616

large-scale networks (after a linearization of function f) is out of the reach of state-of-the-art integer solvers. In theoretical computational complexity, the problem is NP-hard in general. A proof can be obtained from a reduction of the NP-hard minimum-interference frequency assignment problem (FAP) in GSM networks [18]. A sketch of the proof is as follows. Consider function f having a step form with values zero and one, and any instance of minimum-interference FAP (for details of FAP, please see [18]), where the interference values are integers. For the FAP instance, let c_{ih} be the co-channel interference caused by cell i on cell h, $i, h \in \mathcal{C}$, if the two cells use the same channel. It is easy to construct an instance of the FFR problem, such that c_{ih} is the number of cell-edge pixels of h, and, for each of them, the function f is one if and only if the two cells use different sub-bands (channels in the FAP instance). Then, one can verify that, for the recognition version of FAP, there exists a solution having total interference less than or equal to I, if and only if the FFR instance has a total throughput of at least $\sum_{i,h\in\mathcal{C}} c_{ih} - I$. Hence the conclusion.

Despite the similarity between FAP and the FFR sub-band allocation problem, there are a couple of structural differences. Whereas the former attempts to reduce interference between cell pairs without explicitly modeling the service area, FFR targets maximizing throughput of cell-edge zones. Problem (4) also differs from FAP in the non-linearity of the objective function.

In view of the computational complexity of (4) and the objective of applying FFR to large-scale networks, we consider a local search algorithm aimed at finding high-quality solutions time-efficiently. Although the algorithm may give sub-optimal solutions, it is reasonable in view of the problem complexity. Indeed, previous literature on FAP suggests that the type of algorithm gives very satisfactory results [18]. After an initial sub-band allocation is made, local search, based on changing the allocation of the sub-band of every cell and swapping the sub-bands of cell pairs, is used for solution improvement. The local search algorithm for FFR optimization is fast, thus it can be for online or semi-online use when FFR optimization is performed for relatively few cells.

B. Initial Allocation (IA)

In IA, the algorithm goes through the cells one by one. Each cell is allocated one sub-band from $\mathcal{K}$. Once a sub-band is chosen for a cell, the allocation is not modified in this phase. The selection of sub-band maximizes the total cell-edge throughput of the cell under consideration and those that have been allocated sub-bands earlier.

The IA procedure is formalized in Algorithm 1. Each execution of the for-loop starting at line 4 allocates a sub-band to one cell. Sub-band selection is performed with the objective of maximizing the throughput of cell-edge zones having sub-bands allocated, including cell i. Solution update is subsequently conducted (line 13). The computational effort demanded by IA is determined by the total number of pixels forming cell edges, and the number of sub-bands. The latter, however, tends to be in a fairly constant interval, because the loss in bandwidth will outweigh the benefit of interference mitigation if too many sub-bands are created.

Algorithm 1 Initial Allocation

1: **for all** $k \in \mathcal{K}$ **do**
2: $\quad \mathcal{C}_k \Leftarrow \emptyset$
3: **end for**
4: **for** $i = 1$ to C **do**
5: $\quad f^* \Leftarrow 0$
6: $\quad$ **for all** $k \in \mathcal{K}$ **do**
7: $\quad\quad \mathbf{c}' = \mathbf{c}$; $\mathcal{C}'_k = \mathcal{C}'_k \cup \{i\}$
8: $\quad\quad$ **if** $f^* < \sum_{\ell=1}^{i} \sum_{j\in\mathcal{J}_\ell^e} f(SINR_{\ell j}(\mathbf{c}'), j)$ **then**
9: $\quad\quad\quad f^* \Leftarrow \sum_{\ell=1}^{i} \sum_{j\in\mathcal{J}_\ell^e} f(SINR_{\ell j}(\mathbf{c}'), j)$
10: $\quad\quad\quad k^* \Leftarrow k$
11: $\quad\quad$ **end if**
12: $\quad$ **end for**
13: $\quad \mathcal{C}_{k^*} \Leftarrow \mathcal{C}_{k^*} \cup \{i\}$
14: **end for**
15: **return** $\mathbf{c}$

C. Improving FFR Allocation by Local Search (LS)

The optimization algorithm applies local search (LS) to iteratively improve the initial FFR allocation. LS adopts two operators for the generation of alternative allocations (aka as neighborhood in LS): modify and swap.

- The first operator modifies the sub-band allocated to an individual cell. For C cells and K sub-bands, the operator is applied $C(K-1)$ times. Note that if the sub-band of cell i is changed from k to h, throughput will be affected in cells in $\mathcal{C}_k$ and $\mathcal{C}_h$ only.
- For pairs of cells having different sub-bands allocated, the second operator makes a swap of them. The number of possible swaps will not exceed C^2. In practice, it's much lower as cell pairs sharing the same sub-band are not subject to swap. Similar to the first operator, it is sufficient to recompute the throughput of cells in $\mathcal{C}_k$ and $\mathcal{C}_h$, if the swap operation involves sub-bands k and h.

In every iteration, LS evaluates the new FFR patterns resulted from all possible applications of the two operators, and moves to the one giving the largest improvement in average throughput. Typically, the algorithm converges very fast. For the networks used in Section IV, optimizing FFR by LS requires no more than a number of seconds in average.

A formal description of LS is given by Algorithm 2. For each sub-band k and each cell i currently using this sub-band, evaluating the effect of using an alternative sub-band is carried out by the for-loop starting at line 7. For cells having sub-bands other than k, sub-band swapping is performed by the for-loop formed by lines 16–25. For the new allocations generated by LS, throughput is re-calculated for the two sub-bands (denoted by k and h in the algorithm) in lines 10–12 and lines 19–21.

Digital Object Identifier: 10.4108/ICST.WICON2010.8616
http://dx.doi.org/10.4108/ICST.WICON2010.8616

Algorithm 2 Local search for FFR Optimization

repeat
  for all $k \in \mathcal{K}$ **do**
    $f_k \Leftarrow \sum_{i \in \mathcal{C}_k} \sum_{j \in \mathcal{J}_i^e} f(SINR_{ij}(\mathbf{k}), j)$
  end for
  $\delta^* \Leftarrow 0$
  for all $k, h \in \mathcal{K} : k \neq h$ **do**
    for all $i \in \mathcal{C}_k$ **do**
      $\mathbf{c}' \Leftarrow \mathbf{c}$
      $\mathcal{C}'_h \Leftarrow \mathcal{C}'_h \cup \{i\}$; $\mathcal{C}'_k \Leftarrow \mathcal{C}'_k \setminus \{i\}$
      $f'_k \Leftarrow \sum_{\ell \in \mathcal{C}'_k} \sum_{j \in \mathcal{J}_\ell^e} f(SINR_{\ell j}(\mathbf{c}'), j)$
      $f'_h \Leftarrow \sum_{\ell \in \mathcal{C}'_h} \sum_{j \in \mathcal{J}_\ell^e} f(SINR_{\ell j}(\mathbf{c}'), j)$
      $\delta \Leftarrow f'_k + f'_h - (f_k + f_h)$
      if $\delta > \delta^*$ **then**
        $\delta^* \Leftarrow \delta$; $\mathbf{c}^* \Leftarrow \mathbf{c}'$;
      end if
      for all $m \in \mathcal{C}_h : i < m$ **do**
        $\mathbf{c}' \Leftarrow \mathbf{c}$
        $\mathcal{C}'_h \Leftarrow \mathcal{C}'_h \cup \{i\}$; $\mathcal{C}'_k \Leftarrow \mathcal{C}'_k \setminus \{i\}$; $\mathcal{C}'_k \Leftarrow \mathcal{C}'_k \cup \{m\}$; $\mathcal{C}'_h \Leftarrow \mathcal{C}'_h \setminus \{m\}$
        $f'_k \Leftarrow \sum_{\ell \in \mathcal{C}'_k} \sum_{j \in \mathcal{J}_\ell^e} f(SINR_{\ell j}(\mathbf{c}'), j)$
        $f'_h \Leftarrow \sum_{\ell \in \mathcal{C}'_h} \sum_{j \in \mathcal{J}_\ell^e} f(SINR_{\ell j}(\mathbf{c}'), j)$
        $\delta \Leftarrow f'_k + f'_h - (f_k + f_h)$
        if $\delta > \delta^*$ **then**
          $\delta^* \Leftarrow \delta$; $\mathbf{c}^* \Leftarrow \mathbf{c}'$;
        end if
      end for
    end for
  end for
  $\mathbf{c} \Leftarrow \mathbf{c}^*$
until $\delta^* = 0$
return $\mathbf{c}^*$

IV. NUMERICAL ANALYSIS

A. Test Networks and Parameters

We report performance results for two large networks. They represent two cellular network planning scenarios for Berlin and Lisbon, respectively. These data sets are provided by the European Momentum project [19]. The parameter setting is based on an effective downlink bandwidth of 4.5 MHz (i.e., the basic bandwidth block of LTE downlink). In our investigation, cell-center and cell-edge bands are allocated 1.8 and 2.7 MHz, respectively. The allocation of bandwidth to cell center and edge leads to a trade-off between the throughput loss of the former and improvement of the latter. This is a topic in its own right, although it's not the focus here. For FFR, the cell-edge band is further split into a number of sub-bands of equal size. To allow for assessing the potential of FFR, we do not impose a granularity limit (e.g., resource block in LTE) in splitting. In each cell, the total Tx power is evenly distributed on all sub-carriers in the cell-center band and the cell-edge sub-band.

Network size and power parameters are summarized in Table I. FFR has been experimented for three cell-edge scenarios.

TABLE I: Test Network Statistics and Parameter Setting.

Network	Berlin	Lisbon
Number of cells	148	164
Area size (pixels)	22,500	52,500
Pixel size (m^2)	50*50	20*20
Total DL Tx power (dBm)	46	46
UE noise figure (dB)	7	7
Thermal noise (dBm)	-107	-107
Cell edge pilot SINR (dB)	$\leq$ -5/-5.8/-6	$\leq$ -4.4/-5/-6
Number of cells with cell edge	116/83/79	147/127/80

For the Berlin network, these scenarios are created by setting pilot SINR threshold to -5, -5.8, and -6 dB; the resulting cell-edge zones correspond to 8%, 5%, and 2% of the service area, respectively. For the Lisbon network, the thresholds are -4.4, -5, and -6 dB, and the percentage values are 5%, 3%, and 1%. The Shannon formula is used to estimate the throughput of each pixel.

The optimization algorithm is implemented in C++. For both networks, the time required by the algorithm is less than one minute on a HP Compaq 8510p laptop.

B. Optimization of Conventional "reuse-3"

First, we divide the cell-edge band into three sub-bands, similar to the conventional reuse-3 scheme for hexagonally shaped cells. Here, however, "reuse-3" optimization is not the reuse-3 pattern (nor a reuse factor of 3) since there is no frequency allocation pattern to follow for an irregular cell layout. It merely refers to the fact that three sub-bands are created. The algorithm will tell the allocation pattern and how often each sub-band should be reused in order to optimize cell-edge throughput.

Figure 2 shows the throughput under reuse-1 for the Lisbon network. Pilot SINR threshold defining cell edge equals -4.4 dB. The result of optimizing "reuse-3" by our algorithm is illustrated in Figure 3. Both figures display the throughput of cell-edge zones by color level; all other pixels (cell center) are denoted grey. The irregular shape of the cell-edge zones is apparent.

Under reuse-1, the throughput is below 2 Mbps at most of the cell-edge pixels in Figure 2. The average throughput is 1.66 Mbps. Under optimized "reuse-3", the throughput grows significantly, with an average value of 2.77 Mbps. Thus the improvement factor is 1.7. As can be seen from the figures, most cell-edge pixels make a jump in throughput. At the same time, it is worth noticing that the throughput of some pixels has decreased in "reuse-3". This is because average throughput has been used as the performance target.

C. Is Three a Magic Number?

Dividing the cell-edge band into three sub-bands and following a reuse-3 pattern are conceptually optimal for regularly shaped cells. It has been frequently used in the literature to analyze FFR. A natural question to ask is if a division into three sub-bands is also the best choice under realistic radio propagation conditions. Our FFR allocation algorithm can be

Digital Object Identifier: 10.4108/ICST.WICON2010.8616
http://dx.doi.org/10.4108/ICST.WICON2010.8616

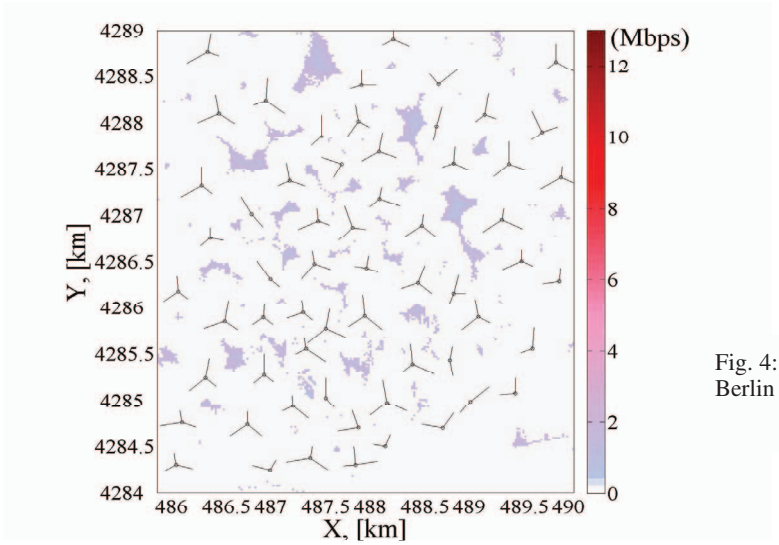

Fig. 2: Cell-edge throughput under reuse-1 for Lisbon.

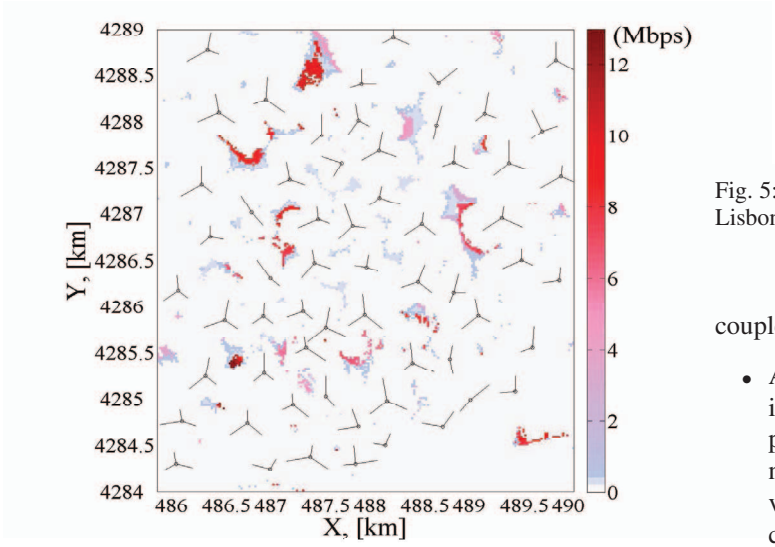

Fig. 3: Cell-edge throughput with optimized "reuse-3" for Lisbon.

used to investigate the aspect as it can work with any number of sub-bands. To this end, the cell-edge band of 2.7 MHz is split into various numbers of sub-bands, ranging from 2 to 10, and the algorithm is applied for each of them. To make a complete comparative study, we perform these experiments for all three pilot SINR threshold values used to define cell-edge zones.

The results are displayed in Figures 4-5 for the Berlin and Lisbon networks, respectively. The curves show the performance improvement by FFR over reuse-1 in average cell-edge throughput. To facilitate comparison, the curves are normalized so the reuse-1 throughput equals to 1.0. (In absolute values, the average cell-edge throughputs under reuse-1 are 1.40, 1.23 and 1.19 Mbps for the Berlin network, respectively, and 1.66, 1.50, and 1.25 Mbps for the Lisbon network, respectively.)

As can be seen clearly from Figures 4-5, the performance improvement factor of FFR over reuse-1 varies significantly by the number of sub-bands and the definition of cell edge. A

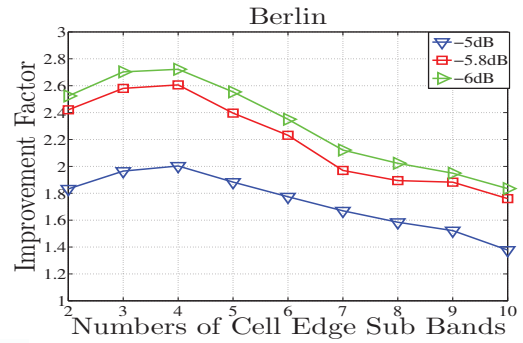

Fig. 4: Normalized improvement factor of cell-edge throughput for the Berlin Network.

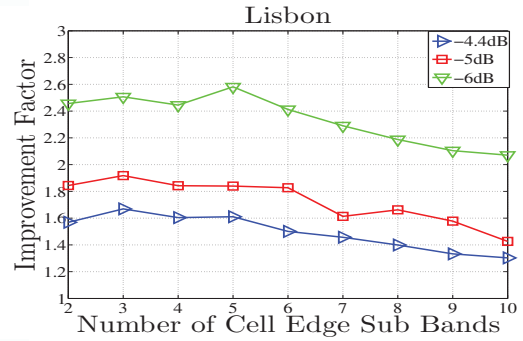

Fig. 5: Normalized improvement factor of cell-edge throughput for the Lisbon Network.

couple of interesting observations follow from the results.

- A partitioning of the cell-edge band into three sub-bands is not necessarily optimal. For the Berlin network, peak performance appears for four sub-bands. For the Lisbon network, three is indeed the best choice for two threshold values, whereas five is optimal when fewer pixels are considered as cell edge. This variation is very much because of the irregular coverage of the cells and the resulting distribution of cell-edge areas.
- As a second observation, performance improvement is very sensitive to the definition of cell edge. A general trend is that improvement due to FFR grows when less pixels are considered to be cell edge. Take Lisbon as an example. With a threshold of -4.4 dB (corresponding to 5% of the entire service area), the peak improvement factor is 1.7. When the threshold is -6 dB (1% of the area) the improvement factor goes up to 2.6. This is because in the latter case, cell edge is formed by areas that are more vulnerable to interference. The performance improvement at cell edge comes with the price of lower throughput in the cell-center zones when compared to reuse-1 (60% for the results in this section). Moreover, although the performance improvement brought by FFR grows when less areas are considered as cell edge, at the same time it means more areas become cell center and have to experience throughput loss. Hence the definition of cell edge must be addressed carefully in practicing FFR.

Digital Object Identifier: 10.4108/ICST.WICON2010.8616
http://dx.doi.org/10.4108/ICST.WICON2010.8616

V. CONCLUSIONS AND FUTURE WORK

We have presented an approach for applying fractional frequency reuse (FFR) in realistic networks with irregularly shaped cells. The approach is based on an optimization algorithm that is designed to maximize the cell-edge throughput of sub-band allocation. The approach not only overcomes the limitation of the conventional schemes, but also enables the adaptation of the number of sub-bands to each individual network. The numerical analysis shows that the approach is applicable to large-scale networks, and the optimization offers significant throughput improvement at cell-edge zones. As a second conclusion, the optimal number of sub-bands varies from one case to another. Moreover, the definition of cell edge heavily influences the performance.

An extension of the current work is FFR with sub-bands of unequal size. Investigation in this direction is underway. Another line of further research is a comparative study between FFR and other reuse schemes for interference mitigation (particularly soft frequency reuse) under realistic cell layout.

ACKNOWLEDGMENT

The work of the first author has been partially financed by CENIIT, Linköping Institute of Technology, Sweden, and the Swedish Research Council (Vetenskapsrådet). The work has been carried out within European COST action 2100.

REFERENCES

[1] Evolved universal terrestrial radio access (E-UTRA), physical channels and modulation. *3GPP TR 36.211, V.8.5.0*, 2008.

[2] Mobile WiMAX-part i: A technical overview and performance evaluation. *WiMAX Forum White Paper*, 2006.

[3] A. Simonsson. Frequency reuse and intercell interference co-ordination in E-UTRA. In *Proceedings of IEEE VTC Spring '07*, pp. 3091–3095, 2007.

[4] Interference mitigation - considerations and results on frequency reuse. R1-050738, *3GPP TSG-RAN WG1 Meeting #42*, 2005.

[5] Inter-cell interference handling for E-UTRA. R1-050764, *3GPP TSG-RAN WG1 Meeting #42*, 2005.

[6] Interference mitigation in evolved UTRA/UTRAN. R1-050833, *3GPP TSG-RAN WG1 Meeting #42*, 2005.

[7] Soft frequency reuse scheme for UTRAN LTE. R1-050507, *3GPP TSG-RAN WG1 Meeting #41*, 2005.

[8] H. Lei, L. Zhang, X. Zhang, and D. Yang. A novel multi-cell OFDMA system structure using fractional frequency reuse. In *Proceedings of IEEE PIMRC '07*, 2007.

[9] Y. Xiang, J. Luo, and C. Hartmann. Inter-cell interference mitigation through flexible resource reuse in OFDMA based communication networks. In *Proceedings of the 13th European Wireless Conference (EWC '07)*, 2007.

[10] X. Mao, A. Maaref, and K. H. Teo. Adaptive soft frequency reuse for inter-cell interference coordination in SC-FDMA based 3GPP LTE uplinks. In *Proceedings of IEEE GLOBECOM '08*, 2008.

[11] R. Y. Chang, Z. Tao, J. Zhang, and C.-C. J. Kuo. A graph approach to dynamic fractional frequency reuse (FFR) in multi-cell OFDMA networks. In *Proceedings of IEEE ICC '09*, 2009.

[12] L. Fang and X. Zhang. Inter-cell interference mitigation through flexible resource reuse in OFDMA based communication networks. In *Proceedings of 4th IEEE International Conference on Wireless Communications, Networking and Mobile Computing (WiCOM '08)*, 2008.

[13] R. Giuliano, P. Loreti, F. Mazzenga, and G. Santella. Fractional frequency reuse planning for WiMAX over frequency selective channels. In *Proceedings of IEEE IWCMC '08*, pp. 666–671, 2008.

[14] M. Assaad. Optimal fractional frequency reuse (FFR) in multicellular OFDMA System. In *Proceedings of IEEE VTC Fall '08*, 2008.

[15] S. H. Ali and V. C. M. Leung. Dynamic frequency allocation in fractional frequency reused OFDMA networks. In *Proceedings of IEEE GLOBECOM Workshops '08*, 2008.

[16] A. L. Stolyar and H. Viswanathan. Self-organizing dynamic fractional frequency reuse in OFDMA systems. In *Proceedings of IEEE INFOCOM '08*, pp. 691–699, 2008.

[17] M. Abaii, G. Auer, F. Bokhari, M. Bublin, E. Hardouin, O. Hrdlicka, G. Mange, M. Rahman, and P. Svac. Interference avoidance concepts. Techical Report, *IST-4-027756 WINNER II, D4.7.2 v1.0*, 2007.

[18] K. Aardal, C. P. M. van Hoesel, A. M. C. A. Koster, C. Mannino, and A. Sassano. Models and solution techniques for the frequency assignment problem. *4OR*, vol. 1, pp. 261–317, 2003.

[19] European project IST-2000-28088, *http://momentum.zib.de*, 2005.

Digital Object Identifier: 10.4108/ICST.WICON2010.8616
http://dx.doi.org/10.4108/ICST.WICON2010.8616